Title: Tunable regioselectivity in 1,3-butadiene polymerization by using 2,6-bis(dimethyl-2-oxazolin-2-yl)pyridine incorporated transition metal (Cr, Fe and Co) catalysts

Author: Dirong Gong Wen Liu Weijing Pan Tao Chen Xiaoyu Jia Kuo-Wei Huang Xuequan Zhang

PII: S1381-1169(15)00186-7
DOI: http://dx.doi.org/doi:10.1016/j.molcata.2015.05.013
Reference: MOLCAA 9499

To appear in: *Journal of Molecular Catalysis A: Chemical*

Received date: 16-2-2015
Revised date: 29-4-2015
Accepted date: 19-5-2015

Please cite this article as: Dirong Gong, Wen Liu, Weijing Pan, Tao Chen, Xiaoyu Jia, Kuo-Wei Huang, Xuequan Zhang, Tunable regioselectivity in 1,3-butadiene polymerization by using 2,6-bis(dimethyl-2-oxazolin-2-yl)pyridine incorporated transition metal (Cr, Fe and Co) catalysts, Journal of Molecular Catalysis A: Chemical http://dx.doi.org/10.1016/j.molcata.2015.05.013

Tunable regioselectivity in 1,3-butadiene polymerization by using 2,6-bis(dimethyl-2-oxazolin-2-yl)pyridine incorporated transition metal (Cr, Fe and Co) catalysts

Dirong Gong[a,b*] gongdirong@nbu.edu.cn, Wen Liu[a], Weijing Pan[a], Tao Chen[b,c], Xiaoyu Jia[e,f], Kuo-Wei Huang[b*] hkw@kaust.edu.sa, Xuequan Zhang[d]

[a]Department of Polymer Science and Engineering, Faculty of Materials Science and Chemical Engineering, Ningbo University, Ningbo 315211, P.R.China.

[b]King Abdullah University of Science and Technology, Division of Physical Sciences and Engineering and KAUST Catalysis Center, Thuwal 23955-6900, Saudi Arabia.

[c]MOE Key Laboratory of Advanced Textile Materials & Manufacturing Technology, National Base for International Cooperation in Science & Technology of Textiles and Daily Chemistry, Zhejiang Sci-Tech University, Hangzhou 310018, P. R. China.

[d]Key Laboratory of Synthetic Rubber, Changchun Institute of Applied Chemistry, Chinese Academy of Sciences, 5625 Renmin Street, Changchun 130022, P. R. China.

[e]Key Laboratory of Urban Environment and Health, Institute of Urban Environment, Chinese Academy of Sciences, No.1799, Jimei Road, Xiamen, Fujian 361021, P. R. China.

[f]Ningbo Urban Environment Observation and Research Station-NUEORS, Chinese Academy of Sciences, Ningbo,Zhejiang 315830, P. R. China.

[*]Corresponding authors.

Graphic Abstract

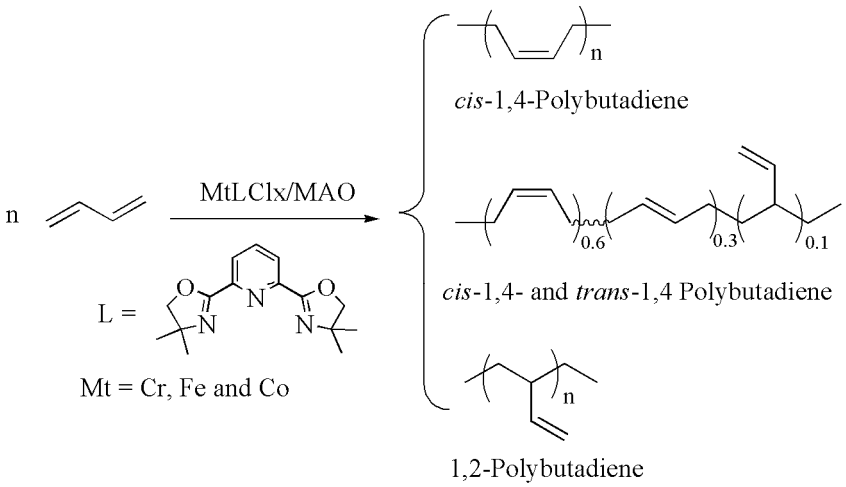

Microstructure Controllable Polymerization of Butadiene

Highlights

Cr(III)L produces 93.3% of *trans*-1,4 selectivity.

Fe(III)L and **Fe(II)L** both show equal *cis*-1,4 and *trans*-1,4 with 10% 1,2 selectivity.

The selectivity from *cis*-1,4 to 1,2 can be tuned by **Co(II)L**.

Controlling of microstructure of polybutadiene is achievable.

Abstract

Tridentate complexes **Cr(III)Cl_3L**, [**L** = 2,6-bis(dimethyl-2-oxazolin-2-yl)pyridine], **Fe(III)Cl_3L**, **Fe(II)Cl_2L** and **Co(II)Cl_2L** have been prepared and fully characterized. The solid structures of **Cr(III)Cl_3L**, **Fe(III)Cl_3L** and **Co(II)Cl_2L** have been revealed by single crystal X-ray diffraction, and the **Cr(III)Cl_3L** and **Fe(III)Cl_3L** complexes both exhibit a distorted octahedral geometry, while the **Co(II)Cl_2L** complex has a trigonal bipyramidal conformation. Four complexes have been examined in regioselective polymerization of butadiene in combination with MAO in toluene at room temperature. The *trans*-1,4, *cis*-1,4 enchainment of resultant polybutadiene are controlled by the metal center. Activated by MAO, complex **Cr(III)Cl_3L** produces high level of *trans*-1,4 selectivity (*trans*-1,4 up to 93.3%) with moderate polymer yield, complexes **Fe(III)Cl_3L** and **Fe(II)Cl_2L** both show equal *cis*-1,4 and *trans*-1,4 with minor 1,2 selectivity (<10%), and **Co(II)Cl_2L** catalyst displays predominated *cis*-1,4 selectivity, which can be shifted to 1,2 selectivity by adding PPh_3 as an additive. Thus, tuning of the *cis*-1,4, *trans*-1,4 and 1,2 selectivity in full range via central metal and additive chosen by these 2,6-bis(dimethyl-2-oxazolin-2-yl)pyridine supported catalysts has been achieved.

Keywords

Transition metal catalysts, 1,3-butadiene, selectivity, 2,6-bis(dimethyl-2-oxazolin-2-yl)pyridine, controllable microstructure

1. Introduction

Of the varieties of elastomers, polybutadiene has been one of the most regarded materials for many practical applications. Stereochemistry in polymerization of butadiene plays a crucial role in determining the mechanical properties and the end use of the materials. The development of new polymerization catalysts for efficient control in chain architectures such as stereochemistry, functionality and chain length in polyconjugated dienes synthese has been one of most active research areas in rubber chemistry as it allows the synthesis of tailor-made polymers with the expected properties.

Traditional free radical and anionic conjugated diene polymerization processed in a random manner resulted in stereoirregular chain microstructure, although recent advances shown precise polymer architecture specified in chain components and length such as block, graft and star polymers based on conjugated dienes and styrene have been achieved via controllable anionic and radical synthetic strategies [1-5]. High level of stereoregulated, but not the molecular weight of conjugated diene polymers can date back to the discovery and emplyment of Z-N type of catalysts since the middle of last century, which has remained one of the widely used organometallic mediated catalytic processes for large production of various rubber based materials. Industry applied systems such as tianium tetraethoxides/$AlEt_3$ [6], vandium trichloride/AlR_3 [7-8], $Co(acac)_3/CS_2$ or Ph_3P [9-10] and recently emerged rare earth catalysts [11,12] are notable for their unique catalytic properties, in particular, polymers with high level of regioregularity such as *trans*-1,4 [11-13], *cis*-1,4 [14-23] and 3,4 (1,2) [24-25] regio- and/or stereoselectivity, as such, 1,2-syndiotactic [23] for polybutadiene, and syndiotactic 3,4 (1,2) [24], isotactic 3,4 [25] for polyisoprene as well as their block combinations have been unprecedently achieved.

Research dedicated to the design and development of homogeneous, single-site catalysts for the synthesis of polydienes during the past twenty years have provided

tremendous momentum in catalyst evolution and have revolutionized the field of polyolefin and polydiene research by establishing new opportunities for mechanistic understanding, catalyst control, and tailored polymer synthesis unachievable for heterogeneous catalyst systems. The infacy of metallocene catalyst has made significant progress with the development of single site group-3, 4 and lanthinide metallocene catalysts [26-30], and this revolution allows us to manipulate polymer microstructures, especially the powerful copolymerization capability of conjugated dienes and various α-olefin monmers furnishing varieties of copolymers with unique chemical and physical properties [31-33]. In paralled to the metallocene revolution, momentous developments have also been witnessed since the discovery of highly active nonmetallocene mid- and late-transition metal polymerization catalysts. Research in this area involves the design of various new ancillary ligands to support and activate the metal center toward diene monomers. In this respect, there has been increasing interests in the applications of N-O [21,34-35], SOOS [31], P-P [36-38], and pincer ligand N,N,X (X = N, P and C) [22,23,39-41] covering over a broad range of catalytic reactions, in particular, catalyzing diene with polar monomers, as such straightforwards access to a new family of functional rubber materials.

We have been establishing pyridine based compounds as ligand family for transition metal catalyzed organic transformations [42-44] and olefin polymerizations [45]. The modification of substituents at proper positions of ligand may conveniently be altered to allow for the fine-tuning of both the steric and electronic properties of ligand, which in turn mediate metal induced catalytic performances. The discovery of bis(arylimino)pyridine ligand assisted olefin catalysts by Brookhart [46] and Gibson [47] have stimulated the evolvement of a great diversity of pincer complexes and many other geometry type of complexes as catalyst precursors over the past two decades. This finding has also intrigued us to investigate the catalytic performance in conjugated diene polymerization and allowed access to various microstructural controlled polybutadienes. The catalyst structure-polymer microstructure relationships show distinctive monomer coordination and insertion modes are operated [48]. In

persuit of efficient catalyst, we also have developed classes of NNN [23] and NNP [42-45] pyridine transition metal olefin and conjugated diene catalysts which have straightforward transformed butadiene to generation of polybutadiene with desired structures. Herein, we report 2,6-bis(dimethyl-2-oxazolin-2-yl)pyridine (Pybox(-Me_2)) supported transition metal complexes for microstructure controllable butadiene polymerization.

2. Results and discussion

2.1. Syntheses and characterization and complexes

Pybox(-Me_2) and the corresponding complexes were prepared with moderate to good yields (Fig. 1). The reaction of metal chlorides with 1.0 equiv. of the ligand in THF overnight under argon atmosphere, followed by removal of the solvent under reduced pressure afforded the corresponding complexes as stable solids. Crystals of four complexes **Cr(III)Cl_3L(C1)**, **Fe(III)Cl_3L(C2)**, **Fe(II)Cl_2L(C3)** and **Co(II)Cl_2L(C4)** obtained from recrystallization in methanol/hexane or diethylether mixtures give satisfactory elemental analyses, mass spectroscopy and IR results all consistent with the expected formula, which are all subject to catalysis. The broad peaks in NMR (CD_3OD as solvent), however, are unable to give additional structural information due to the paramagnetic properties of all four complexes. Crystals of complexes **Cr(III)Cl_3L**, **Fe(III)Cl_3L** and **Co(II)Cl_2L** suitable for X-ray diffraction were obtained at -30 °C by double-layering methanol or DMF solutions of the complexes either with n-hexane or diethyl ether. The crystal data and structure refinements of complexes were listed in Table 1.

The differences in metal center do not lead to the significant distinction in their crystal and molecular structure. Single crystal X-ray structure analyses of **Cr(III)Cl_3L** (Fig. 2) and **Fe(III)Cl_3L** (Fig. 3) complexes are both crystallized in orthorhombic system and Pnma space group. They have an identical molecular structure with three

coordinated nitrogen atoms and three coordinated chlorides, and the geometry at the metal center is a little distorted from the typical octahedral geometry. The whole molecule displays C_{2v} symmetry about the equatorial plane with the other two nitrogens situated on the ends of the bent axis, in consistent with the decribed six coordinated iron and chromium complexes [22,23]. As seen from the crystal structure, the coordination of three chlorides builds an equatorial plane approximately vertical to the plane defined by three chelating nitrogens. The metal pyridinyl nitrogen bond (Mt-N1, Mt denotes Cr and Fe) is shorter than the corresponding two Mt-N (Pybox(-Me_2)) bonds in both Cr and Fe complexes, with Cr-N2 (2.039(2) Å and 2.0856(17) Å) having a remarkably shorter distance than the analogous bond Fe-N2(2.169(2) Å, 2.1655(15) Å), implying a contracted ionic radius of chromium (III). The metal and *trans*-chloride bond distance (with respect to pyridinyl nitrogen) is generally less than the other metal-chloride bonds, while the bond value of Cr-Cl2 (2.2907(8) Å) is slightly more than the corresponding Fe1-Cl2 (2.2539(8) Å). A relatively open coordinative environment constructed surrounding the chromium metal center can be observed from the smaller N1-Cr1-N1A (153.48(10)^o) angle compared to analogous N1-Fe1-N1A 146.62(9)^o.

The crystallographic analysis reveals that the **Co(II)Cl_2L** (Fig. 4) is a typical five-coordinated complex with pseudo-trigonal bipyramidal configuration about the cobalt center with tridentated nitrogens and two chlorides moieties. The pyridinyl nitrogen atom and two chlorides compose an equatorial plane, with the sum of three equatorial angles (119.79(3)^o, 139.43(5)^o and 100.77(5)^o) being 359.99^o, indicative of the central metal located exactly on the plane, and the Co-N2 and Co-N3 occupying the apical position with forming a subtended angle N2-Co-N3 of 147.89(7)^o. The Cl1-Co-Cl2 is 119.79(3) ^{o} and N1-Co-N2 is 147.89(7) ^{o}, which are very close to values of the five coordinated cobalt dichloride complexes.

Generally, the parameters of metal-nitrogen and metal-chloride bonds vary with the electron status of the central metal Cr(III) (d^3), Fe(III) (d^5) and Co(II) (d^7), with average distance changing in the order of Co(II)-N(2.168Å) > Fe(III)-N (2.167Å) > Cr(III)-N (2.070Å) and Fe(III)-Cl(2.312Å), Cr(III)-Cl (2.312Å) > Co(II)-Cl(2.282Å). These subtle structures may affect their catalytic performance by influencing the monomer orientation, coordination mode, insertion into the growing polymer as well as the interconversion of *syn*-ally between *anti*-ally intermediate isomers.

2.2. The tunability of the selectivity

2,6-bis(oxazolin-2-yl)pyridines are versatile ligands assisted in metal catalysts for various organic transformation due to their feasible syntheses and easy modification of the steric and electronic properties, in particular, adjusting enantioselectivity via introducing chiral center into appropriate place of ligand has led to tremendous efficient chiral catalysts for organic building [49-52]. Description of their catalysis behavior for polymerization, however, is conspiculously less, and reported examples are only limited in chromium [53], iron [54] and ruthenium catalysts [55].

The polymerization results in this study are described including the effects of various catalyst and polymerization parameters such as metal center, cocatalyst and additive. The polymerization conditions and polymer analysis results were complied in Table 2. Discussion of the experiment data in addition to the relation between catalytic performance and catalyst structure are also conducted, which could allow us to explore potential efficient catalysts. We begin our study with MAO as cocatalyst, as it has been demonstrated as a versatile activator in later transition metal catalyzed conjugated diene polymerization. It is worth noting, under identical conditions, blank experiments carried out with $CrCl_3$/MAO, $FeCl_3$/MAO and $FeCl_2$/MAO alone show their inability to polymerize butadiene, while we did observe slow polymerization process with an estimated 20% in polymer yield and 92% *cis*-1,4 selectivity for $CoCl_2$/MAO heterogeneous catalyst [48]. Herein, we examine with MAO/MtL (Mt = $CrCl_3$, $FeCl_3$, $FeCl_2$ and $CoCl_2$, L = Pybox(-Me_2)) at value of 300 and 600. On the

basis of the ^{13}C NMR and IR analysis, microstructures in the resultant polymers were calculated and the data were also given in Table 2. Interestingly, the Pybox(-Me_2) ligated transition metal catalysts/MAO shows a markable sensitivity to the central metal of catalyst. Chromium catalyst is basically favorable for *trans*-1,4 selectivity of 93.3% (table 2, run 1), consistent with that of chromium analogue reported [53]. Of note is that an identical performance observed: a moderate *trans*-1,4 selectivity (59.5% and 55.6%, respectively) and *cis*-1,4 selectivity (30.5% and 32.6%, respectively) has been found for iron(III) (table 2, run 3) and iron(II) (table 2, run 5) catalysts, implying similar active centers involved in catalysis after activation by MAO, while cobalt catalyst displays a typical *cis*-1,4 selectivity (95.3%) (table 2, run 7). This switchable selectivity induced by the metal centers can be elucidated by diene mechanism developed by Tobisch [57,58]. Our publications [23,48] relating to bisiminopyridine ligated iron, cobalt and nickel catalyzed butadiene polymerization have also proposed the possible reaction mechanism operated in the *cis*-1,4, *trans*-1,4 and 1,2 polymerizations and polymerization performances here indicate the analogous reaction mechanism is operated by tridentated ligand in the present catalyst system. It is assumed that at the initial stage, the reaction of complexes with Me-abstracting MAO reagent forms a cationic species of the type $[LMtMe]^+$, and the generated vacant site is opening available for monomer either via *trans*-η^2 or *cis*-η^4 coordination mode. In case of Cr catalyst, the *trans*-η^2 coordinated monomer inserts into the Cr-alkyl bond forming *allyl* coordinated terminal group which takes preferably a thermal stable *syn*-conformation, affording *trans*-stereoregulated growing polymer chain. Considering one coordination bond (Co-$N_{pybox(-Me2)}$) is likely to cleavage [48] for generating cobalt active species, *cis*-η^4 coordination mode thus is assumed, and the formed *anti-allyl* configurated polymer chain ultimately lead to a kinetic favored *cis*-1,4 product. While for two Fe catalysts, due to the 16e characteristic of cationic iron center, *trans*-η^2 coordination of monomer to metal center could be considered first, in case of monomer insertion rate is comparable with the isomerization arrangement of *syn-allyl* iron species to *anti-allyl* configuration, a comparable *cis*-1,4

and *trans*-1,4 enchained product tends to be generated. This isomerization mechanism proceeding with retention or inversion of one configuration is of upmost importance when addressing stereospecific polymerization of butadiene.

However, adjusting MAO addition (Al/Co = 300 or 600) amount does not effect the selectivity significantly, and slightly influences on the polymer yield only. By GPC analysis, molecular weight of ten-thousand of magnitude and a polydispersity index (PDI) of 2-3 is calculated, implying single site active species are generated.

2.3. The temperature and cocatalyst effect on catalytic performance of ***Co(II)Cl$_2$L***

Cis-1,4 polybutadiene is well-known for the excellent low abrasion and low heat building, and of particular interest is a slightly increased *cis*-1,4 percentage of high *cis*-1,4 polybutadiene (>98%) usually brings about a prominent stress induced crystallization which improves the mechanic properties significantly. Herein, we are examing the **Co(II)Cl$_2$L** catalyzed *cis*-1,4 selective polymerization in detail. A temperature-dependent study is performed first for **Co(II)Cl$_2$L**. At a precatalyst loading of 0.1 mmol and employing 30 mmol of MAO, an optimized polymer yield of 75.2% is recorded at room temperature with a number molecular weight (M_n) of 11.6×10^4 (table 3, run 13). Compared with that under room temperature, the poor efficiency of the catalytic system is both found at 0 ^oC (table 3, run 8) andat 38 ^oC with almost no effect on M_n and selectivity (table 3, run 9), however, when increasing temperature to 55 ^oC (table 3, run 10), polymer yield has decreased significantly, concurrent with decreased molecular weight and increased polydispersity index. Employing the optimized polymerization temperature, results for various cocatalysts activated cobalt catalyst for butadiene polymerization were tabulated in Table 3 (run 14-20). We examine the optimal operative cocatalyst for this study. Cocatalysts MAO, triisobutyl aluminum (TIBA), $Ph_3C^+[B(C_6F_5)_4]^-$ and ethyl aluminum chlorides are selected and studied here for catalyst **Co(II)Cl$_2$L**. We begin our cocatalyst studies from low MAO excess ratios, a polymer yield about 47.4% is observed at MAO/Co = 100 (run 11 in table 3). Run 12-13 in table 3 show that both the polymer yield and M_n of the polymers reaching maximum values at MAO/Co = 300, and the produced

polymers possess a very low PDI. Of note is that the selectivity is varied significantly, and it is found to be mainly *trans*-1,4 about 93.3% at MAO/Co = 100, 95.3 % *cis*-1,4 at value of 300, and increased to 96.6% at 600. Presumably, the generated active species (at low MAO/Co =100) favors *trans*-η^2 coordination with monomer, thus producing *trans*-1,4 polymer. In the case of MAO/Co = 300 or 600, one of Co-N bond is likely to diassociate by nucleophilic attack from excess of MAO, and the monomer tend to coordinates with metal by *cis*-η^4 mode, as one more vacant site is available for binding, therefore, *cis*-1,4 polymer is produced. These results indicate MAO amount has ability to control the M_n of polymers by chain transfer to aluminium and the selectivity without major critical changes polymer yield. Tested with TIBA, it is observed that this cocatalyst is virtually inactive towards butadiene, however addition of $Ph_3C^+[B(C_6F_5)_4]^-$ results in an active catalyst for butadiene polymerization, with moderate activity and improved *cis*-1,4 selectivity. The increased activity indicates that the combined addition of TIBA and $Ph_3C^+[B(C_6F_5)_4]^-$ is responsible for a synergetic catalytic property, producing more active cationic center, rather than mere action as an oxygen and moisture scavener agent for TIBA. The more Lewis acidic $AlEt_2Cl$ and $Al_2Et_3Cl_3$ are tested and found to be superior to MAO, and TIBA/$Ph_3C^+[B(C_6F_5)_4]^-$on polymer yield and *cis*-1,4 specific selectivity, indicative of the generated more acidic cationic species is mainly responsible for accelerated monomer coordination, insertion and thus chain propogation. It is also significant that $AlEt_2Cl$ and $Al_2Et_3Cl_3$ increase the electronic deficiency of the cationic $LCoR^+$, enhance electrophilicity at the metal center and facilitate butadiene binding and activation, ultimately leading to an increased catalytic activity. Interestingly, the M_n and PDI of all polymers remain a relatively narrow with range from 1.9-2.7, virtually independent of the nature of cocatalysts.

2.4. The tunable selectivity of ***Co(II)Cl$_2$L***

Tuning the catalytic selectivity *in situ* is an efficient method for simultaneously realizing varieties of polymers based on one catalyst system, to reach this goal, various strategies including elaboration of ligand structure, central metal chosen, polymerization parameters screening such as temperature, cocatalyst and solvent as well as addition of additive have been reported. The importance of additive used mainly arised from powerful tuning ability, as well as their commercial availability, avoiding elaborate multi-step synthesis, which allow straightforward to useful industrial catalyst recipes. Cobalt catalysts are well-known for versatile selectivities as the catalytic performance can be well controlled by the catalyst components and polymerization parameters [21-23,38]. Herein, we investigate the selectivity under preexamined conditions by adding π-donor PPh_3. Introducing 0.1 equiv. of Ph_3P increases the polymer yield and 1,2-selectivity, though the typical *cis*-1,4 selectivity is intact. Generally, increasing of PPh_3 leads to increasing in polymer yield and 1,2 selectivity (run 22-24). The dramatic selectivity changing from 96% of 1,4- up to 83.6 % for 1,2-enchainment with the use of 1.0 equivalent of PPh_3 indicates the insertion mechanisms are significantly influenced by the use of phosphine containing additives, which results in a 1,2-insertion instead of 1,4-insertion. Also, the selectivity and the polymer yields are related to the phosphine feeding amount, both values reaching a pleatu at P/Co = 1.0, and further increase feeding does not observe significant additional increases (table 3, run 24-26) in Table 4. This means 1.0 equivalent of phosphine is required to occupy the one vacant site, thus making *trans*-η^2 rather than *cis*-η^4 coordination of monomer to metal center possible, and the subsequent C3 insertion leads to a 1,2 rich enchainment [23,57]. Interestingly, addition of σ-donor PEt_3 or PCy_3 (table 3, run 27,28) to the cobalt catalyst leads to only a slightly increased 1,2 selectivity, with 1,2 percentage of 17.1% and 28.4%, respectively, suggestive of the less importance of σ-nature of additive to 1,2 insertion [58]. Gel permeation chromatography (GPC) analyses on the resultant polymers by these catalysts show polymers have relative high molecular weight and basically unimodal and narrow PDI, keeping a characteristic for the single-site nature of these

catalyst systems.

In summary, we have prepared and characterized Pybox(-Me_2) supported chromium, iron and cobalt butadiene catalysts. Feasible controlling of polymer microstructure from *cis*-1,4 to *trans*-1,4 has been realized via metal chosen, and controlling of 1,2 and *cis*-1,4 percentage within wide range have also been achieved by adding additive PPh_3 in cobalt catalyst.

4. Experimental

4.1. General methods

All experiments that required inert atmosphere were performed under argon using a Braun Labmaster drybox or standard Schlenk line techniques. 2,6-(chloromethyl)pyridine, 2-amino-2-dimethylpropanol and phosphines were purchased from Alfa Aesar. Methylaluminoxane, Al^iBu_3, $AlEt_2Cl$, $Al_2Et_3Cl_3$ and $Ph_3C^+[B(C_6F_5)_4]^-$ were purchased from AkzoNoble and Strem. All solvents were purified by standard methods. Polymerization grade 1,3-butadiene was purified by $AlEt_3$ prior to use. Deturated solvents were purchased from Cambridge Isotope Laboratories, Inc., degassed, and dried over activated 4 Å molecular sieves prior to use. Ligand was synthesized by our reported method [59]. NMR analyses of ligands and polymers were performed on a Bruker spectrometer, and the microstructures of polybutadiene were calculated by our reported methods [48]. IR spectra of ligands were recorded on a BRUKE Vertex-70 FIR spectrophotometer. Elemental analyses for carbon, nitrogen and hydrogen were carried out with an elemental Vario EL spectrometer. ICP-MS analyses for chromium, iron and cobalt were run by Agilent 7500cx after microwave digestion with concentrated HCl. The molecular weights (M_w and M_n) and the molecular weights distributions (M_w/M_n) of polymer samples were measured by VISCOTEK GPC1000 with TDA305 (Triple Detector Array) as detector at 30 °C using THF as the solvent at a flow rate of the eluent of 1 mL/min, calibrated by narrow polystyrene standards.

4.2. X-ray structure determinations

Single crystals subject to analysis were grown by diffusion of hexane or diethyl ether to a saturated methanol or dichloromethane solution containing the corresponding complexes. X-ray analysis data were collected on a Bruker SMART APEX diffractometer with a CCD area detector, using graphite monochromated Mo K radiation (λ = 0.71073 Å). Crystal class and unit cell parameters were determined by the SMART program package. Reflection data file was yielded from raw frame data by SAINT and SADABS and the structures were solved based on SHELXTL program. Refinement was processed on F^2 anisotropically for all non-hydrogen atoms by the full-matrix least-squares method.

CCDC reference numbers 1005508 and 1005506, 1005507 are for complexes **Cr(III)Cl_3L**, **Fe(III)Cl_3L** and **Co(II)Cl_2L**, respectively.

4.3. Syntheses and characterization of complexes

[2,6-Bis(dimethyl-2-oxazolin-2-yl)pyridine]chromium trichloride (**Cr(III)Cl_3L**)

To a suspension of $CrCl_3(THF)_3$ (750 mg, 2 mmol) in THF (5 mL) was added a THF (10 mL) solution of ligand 2,6-bis(dimethyl-2-oxazolin-2-yl)pyridine (599 mg, 2.2 mmol). A green suspension was formed after about 2h at room temperature, and further stirred overnight was required to complete the reaction. A green solid (1.08 g, 80% in yield) was finally collected by filtration, washed with diethyl ether (10 mL × 3) and drying. The other complexes **Fe(III)Cl_3L-Co(II)Cl_2L** were prepared by the similar method.

Yield: 80%. IR (KBr, cm^{-1}): 1620 ($\nu_{C=N}$). Anal. Calc. for $C_{15}H_{19}Cl_3CrN_3O_2$: C, 41.73; H, 4.44; N, 9.73. Found: C, 41.31; H, 4.53; N, 9.67 %. Cr: 12.04% (Calc.12.19%). MS (ESI): m/z 396.3, $[M\text{-}Cl]^+$(100%); 428.2 $[M\text{-}Cl+CH_3OH]^+$(14%).

[2,6-Bis(dimethyl-2-oxazolin-2-yl)pyridine]iron trichloride (**Fe(III)Cl_3L**), Yield: 92.3%. IR (KBr, cm^{-1}): 1620 ($\nu_{C=N}$). Anal. Calc. for $C_{15}H_{19}Cl_3FeN_3O_2$: C, 41.37; H, 4.40; N, 9.65. Found: C, 41.37; H, 4.48; N, 9.47 %. Fe: 12.82% (Calc.13.07%). MS (ESI): m/z 400.1, $[M\text{-}Cl]^+$(28%); 432.2 $[M\text{-}Cl+CH_3OH]^+$(100%).

[2,6-Bis(dimethyl-2-oxazolin-2-yl)pyridine]iron dichloride (**Fe(II)Cl_2L**), Yield: 97.1%. IR (KBr, cm^{-1}): 1620 ($\nu_{C=N}$). Anal. Calc. for $C_{15}H_{19}Cl_2FeN_3O_2$: C, 45.03; H,

4.79; N, 10.50. Found: C, 44.87; H, 4.88; N, 10.67 %. Fe: 13.96% (Calc.14.09%). MS (ESI): m/z 400.1, $[M]^+$(43%); 432.2 $[M+CH_3OH]^+$(100%).

[2,6-Bis(dimethyl-2-oxazolin-2-yl)pyridine]cobalt dichloride (**Co(II)Cl_2L**), Yield: 94.6%. IR (KBr, cm^{-1}): 1620 ($\nu_{C=N}$). Anal. Calc. for $C_{15}H_{19}Cl_2CoN_3O_2$: C, 44.69; H, 4.75; N, 10.42. Found: C, 44.77; H, 4.91; N, 10.59%. Co: 14.62% (Calc.14.87%). MS (ESI): m/z 403.17, $[M]^+$(100%); 432.2 $[M-Cl+CH_3OH]^+$(32%).

4.4. Procedure for butadiene polymerization

The polymerization runs were carried out following a standard procedure. A 100 mL flask equipped with a magnetic bar was charged with cocatalyst and butadiene solution (0.58 g, 0.0108 mol) in toluene (15 mL). After equilibration of the solution at the polymerization temperature the reaction was started by injection of a toluene suspension (5 mL) of **Cr(III)Cl_3L** (8 mg, 12.5 mol). The polymerization then was terminated after a given time by introducing acidified ethanol (15 mL, 0.5 % HCl) containing 1.0% 2,6-di-tert-butyl-4-methyl phenol as an antioxidant. The polymer was coagulated in acidified ethanol (20 mL, 0.5 % HCl), recovered by filtration, washed with an excess of ethanol and dried in vacuo at room temperature to a constant weight for subsequent characterization. The polymer yield was calculated based on the monomer loading and polymer weight.

Acknowledgment:

This work is supported by the Natural Science Foundation of China (Grant No. 21304050), Natural Science Foundation of Ningbo (Grant No. 2014A610109), Natural Science Foundation of Fujian Province (Grant No. 2015H0045) and sponsored by K. C. Wong Magna Fund in Ningbo University.

References

[1] T. Higashihara, M. Hayashi, A. Hirao, Prog. Poly. Sci. 36 (2011) 323-375.

[2] V. Jitchum, S. Perrier, Macromolecules 40 (2007) 1408-1412.

[3] I. Natori, S. Inoue, Macromolecules 31 (1998) 982-987.

[4] N. Hadjichristidis, M. Pitsikalis, S. Pispas, H. Iatrou, Chem. Rev. 101 (2001) 3747-3792.

[5] N. Ajellal, C. M. Thomas, J. Carpentier, Polymer 49 (2008) 4344-4349.

[6] P. H. Moyer, M. I. Lehr, J. Polym. Sci. Part A (1965) 217-229.

[7] J. S. Lasky, H. K. Garner, R. E. Ewart, Ind. Eng. Chem. Prod. Res. Dev. 1 (1962) 82-85.

[8] E. Colamarco, S. Milione, C. Cuomo, A. Grassi, Macromol. Rapid Commun. 25 (2004) 450-454.

[9] H. Ueno, K. Oizumi, H. Ishikawa, K. Nakajima, N. Tsujimoto, O. Kimura, H. Aikwa, U. S. Patent (1979) 4153767.

[10] H. Ashitaka, K. Jinda, H. Ueno, J. Polym. Sci. Polym. Chem. Ed. 21 (1983) 1951-1972.

[11] S. Kaita, M. Yamanaka, A. Horiuchi, Y. Wakatsuki, Macromolecules 39 (2006) 1359-1363.

[12]D. Robert, T. P. Spaniol, J. Okuda, Eur. J. Inorg. Chem. (2008) 2801-2809.

[13]R. Taube, S. Maiwald, J. Sieler, J. Organomet. Chem. 621 (2001) 327-336.

[14]X. Li, J. Baldannis, M. Nishiura, O. Tardif, Z. Hou, Angew. Chem. Int. Ed. 45 (2006) 8184-8188.

[15] L. Zhang, T. Suzuki, Y. Luo, M. Nishiura, Z. Hou, Angew. Chem. Int. Ed. 46 (2007) 1909-1913.

[16] W. Gao, D. Cui, J. Am. Chem. Soc. 130 (2008) 4984-4991.

[17] K. Endo, Y. Yamanaka, Macromol. Rapid Commun. 20 (1999) 312-314.

[18] L. Porri, G. Ricci, N. Shubin, Macromol. Symp. 128 (1998) 53-61.

[19] R. Cariou, J. Chirinos, V. C. Gibson, G. Jacobsen, A. K. Tomov, M. R. J. Elsegood, Macromolecules 42 (2009) 1443-1444.

[20] L. Porri, M. Aglietto, Makromol. Chem. Macromol. Chem. Phys. 177 (1976) 1465-1476.

[21] D. Gong, B. Wang, X. Jia, X. Zhang, Dalton Trans. 43 (2014) 4169-4178

[22] D. Gong, B. Wang, H. Cai, X. Zhang, L. Jiang, J. Organomet. Chem. 696 (2011) 1584-1590.

[23] D. Gong, W. Jia, T. Chen, K.-W. Huang, Appl. Catal. A: Gen. 464-465 (2013) 35-42.

[24] B. Wang, D. M. Cui, K. Lv, Macromolecules 41 (2008) 1983-1988.

[25] L. Zhang, Y. Luo, Z. Hou, J. Am. Chem. Soc. 127 (2005) 14562-14563.

[26] S. Kaita, Z. Hou, M. Nishiura, Y. Doi, J. Kurazumi, A. C. Horiuchi, Y. Wakatsuki, Macromol. Rapid Commun. 24 (2003) 180-184.

[27] L. A. Van der, J. C. Schaverien, N. Meijboom, C. Ganter, A. G. Orpe, J. Am. Chem. Soc. 117 (1995) 3008-3021.

[28] A. Miyazawa, T. Kase, K. Soga, Macromolecules 33 (2000) 2796-2800.

[29] H. T. Ban, Y. Tsunogae, T. Shiono J. Polym. Sci. Part A: Polym. Chem. 42 (2004) 2698-2704.

[30] W. Kaminsky, B. Hinrichsa, D. Rehderb, Polymer 43 (2002) 7225-7229.

[31] C. Capacchione, A. Avagliano, A. Proto, Macromolecules 41 (2008) 4573-4575.

[32] S. Milione, C. Cuomo, C. Capacchione, C. Zannoni, A. Grassi, Macromolecules 40 (2007) 5638-5643.

[33] J. Dassaud, A. Guyot, R. Spitz, Makromol. Chem. 194 (1993) 2631-2639.

[34] D. Chandran, C. H. Kwak, C.-S. Ha, I. Kim, Catal. Today 131 (2008) 505-512.

[35] K. Endo, T. Kitagawa, K. Nakatani, J. Polym. Sci. Part A: Polym. Chem. 44 (2006) 4088-4094.

[36] G. Ricci, M. Battistella, Macromolecules, 34 (2001) 5766-5769.

[37]G. Ricci, A. Forni, A. Boglia, M. Sonzogni, Organometallics 23 (2004) 3727-3732.

[38] G. Ricci, A. Forni, A. Boglia, A. Sommazzi, F. Masi, J. Organomet. Chem. 690 (2005) 1845-1854.

[39] R. Cariou, J. J. Chirinos, V. C. Gibson, G. Jacobsen, A. K. Tomov, G. J. P. Britovsek, A. J. P. Whitea, Dalton Trans. 39 (2010) 9039-9045.

[40] R. Cariou, J. Chirinos, V. C. Gibson, G. Jacobsen, A. K. Tomov, M. R. J. Elsegood, Macromolecule 42 (2009) 1443-1444.

[41] V. Appukuttan, L. Zhang, C. Ha, I. Kim, Polymer, 2009, 50, 1150-1158.

[42] L. He, T. Chen, D. Gong, Z. Lai, K.-W. Huang, Organometallics 31 (2012) 5208-5211.

[43] T. Chen, L. He, D. Gong, L. Yang, X. Miao, K.-W. Huang, Tetra. Lett. 53 (2012) 4409-4412;

[44]L. He, T. Chen, D. Xue, M. Eddaoudi, K.-W. Huang, J. Organomet. Chem. 700 (2012) 202-206.

[45] D. Gong, W. Liu, T. Chen, Z, Chen, K.-W. Huang, J. Mole. Catal. Chem. 395 (2014) 100-107.

[46] B. L. Small, M. Brookhart, A. M. A. Bennett. J. Am. Chem. Soc. 120 (1998) 4049-4050.

[47] G. J. P. Britovsek, M. Bruce, V. C. Gibson, B. S. Kimberley, P. J. Maddox, S. Mastroianni, J. Am. Chem. Soc. 121 (1999) 8728-4870.

[48] D. Gong, B. Wang, C. Bai, J. Bi, F. Wang, W. Dong, L. Jiang, X. Zhang, Polymer 50 (2009) 6259-6264.

[49] D. A. Evans, Z. K. Sweeney, T. Rovis, J. S. Tedrow, J. Am. Chem. Soc. 123 (2001) 12095-12096.

[50] J. Wang, M. Frings, C. Bolm, Angew. Chem. Int. Ed. 52 (2013) 8661-8665.

[51] A. B. Kazi, G. D. Jones, D. A. Vicic, Organometallics 24 (2005) 6051-6054.

[52] P. J. Heard, C. Jones, J. Chem. Soc. Dalton Trans. (1997) 1083-1088.

[53] Y. Nakayama, K. Sogo, Z. Cai, H. Yasuda, T. Shiono, Polym. Int. 60 (2011) 692-697.

[54] J. Guo, B. Wang, J. Bi, C. Zhang, H. Zhang, C. Bai, Y. Hu, X. Zhang, Polymer 59 (2015) 124-132

[55] K. Nomura, S. Warit, Y. Imanishi, Bull. Chem. Soc. Jpn. 73 (1999) 599-605.

[56] K. Nomura, S. Warit, Y. Imanishi, Macromolecules 32 (1999) 4732-4734.

[57] S. Tobisch, Canadian J. Chem.-Revue Canadienne De Chimie 87 (2009) 1392-1405.

[58]Y.C. Jang, P.S. Kim, H. Lee, Macromolecules 35 (2002) 1477-1480.

[59] T. Chen, L. Yang, D. Gong, K.-W. Huang, Inorg. Chim. Acta 423 (2014) 320-325.

Figure captions

Fig. 1 2,6-Bis(dimethyl-2-oxazolin-2-yl)pyridine supported **Cr(III)Cl_3L**, **Fe(III)Cl_3L**, **Fe(II)Cl_2L** and **Co(II)Cl_2L** complexes

Fig. 2 ORTEP drawing of complex **Cr(III)Cl_3L** with thermal ellipsoids at 30% probability level. Hydrogen atoms have been omitted for clarity.

Fig. 3 ORTEP drawing of complex **Fe(III)Cl_3L** with thermal ellipsoids at 30% probability level. Hydrogen atoms have been omitted for clarity.

Fig. 4 ORTEP drawing of complex **Co(II)Cl_2L** with thermal ellipsoids at 30% probability level. Hydrogen atoms have been omitted for clarity.

Tables

Table 1 Crystal data and structure refinements of complexes **Cr(III)Cl_3L**, **Fe(III)Cl_3L** and **Co(II)Cl_2L.**

	Cr(III)Cl_3L	**Fe(III)Cl_3L**	**Co(II)Cl_2L**
Formula	$C_{15}H_{19}Cl_3CrN_3O_2$	$C_{15}H_{19}Cl_3FeN_3O_2$	$C_{15}H_{19}Cl_2Co_1N_3O_2$
Molecular weight	431.68	435.53	403.16
Crystal system	orthorhombic	orthorhombic	monoclinic
Space group	Pnma	Pnma	P21/C
a (Å)	17.6621(4)	17.7708(4)	10.1419(2)
b (Å)	8.4656(2)	12.7778(3)	15.7789(4)
c (Å)	12.6468(3)	8.3375(2)	11.2958(3)
α (deg)	90.00	90.00	90.00
β (deg)	90.00	90.00	98.996(2)
γ (deg)	90.00	90.00	90.00
V ($Å^3$)	1890.95(8)	1893.21(8)	1785.41(7)
Z	4	4	4
D_{calcd} (Mg/m^3)	1.544	1.561	1.500
Absorp coeff (mm^{-1})	1.008	1.220	1.271
F(000)	10318	13360	828
Crystal size(mm)	0.33×0.21×0.21	0.29×0.20×0.11	0.33×0.21×0.18
θ Range (deg)	1.02 to 26.33	1.02 to 26.33	0.86 to 26.03
No. of reflns collected	7256	7501	9891
No. of indep reflns	2384 (R_{int} = 0.0293)	2396 (R_{int} = 0.028)	4282 (R_{int} = 0.0283)
No. of data/restraint /params	2384/0/120	2396/0/120	4282/0/212
GOF on F^2	1.085	1.069	1.052
R_1(I>2sigma(I))	0.0368	0.0333	0.0353
wR_2	0.0830	0.0704	0.0745

Table 2 The tunable selectivity of Pybox(-Me_2) ligated **Cr(III)Cl_3L**, **Fe(III)Cl_3L,** **Fe(II)Cl_2L** and **Co(II)Cl_2L** catalysts

Run	Precursor	[MAO]/ [Mt]	Yield (%)	Microstructure (%)			M_n (10^4)	PDI
				Trans-1,4	*Cis*-1,4	1,2		
1	**Cr(III)Cl_3L**	300	47.4	93.3	4.9	1.8	1.6	1.9
2	**Cr(III)Cl_3L**	600	53.2	91.9	6.7	1.4	-	-
3	**Fe(III)Cl_3L**	300	37.0	59.5	30.5	10.0	2.9	2.5
4	**Fe(III)Cl_3L**	600	42.1	60.4	31.6	8.0	-	-
5	**Fe(II)Cl_2L**	300	56.9	55.6	32.6	11.2	3.1	2.9
6	**Fe(II)Cl_2L**	600	48.9	57.8	30.7	11.5	-	-
7	**Co(II)Cl_2L**	300	75.2	3.5	95.3	1.2	11.6	2.7

Polymerization conditions: toluene, 20 mL; butadiene, 0.1 mol; precursor, 0.05 mmol; 25 ^oC, polymerization time, 4h.

Table 3 The performance of **Co(II)Cl_2L** catalyzed *cis*-1,4 selective polymerization

Run	Cocatalyst	[Al]/ [Mt]	Yield (%)	Microstructure (%)			M_n (10^4)	PDI
				Trans-1,4	*Cis*-1,4	1,2		
8	MAO	300[a]	47.8	3.4	95.8	0.8	9.0	1.7
9	MAO	300[b]	72.6	3.0	94.7	2.3	9.6	2.2
10	MAO	300[c]	23.1	5.2	92.7	2.1	9.9	2.2
11	MAO	100	47.4	93.3	4.9	1.8	5.6	1.9
12	MAO	300	75.2	3.5	95.3	1.2	11.6	2.7
13	MAO	600	56.9	2.4	96.6	1.2	6.1	2.9
14	Al^iBu_3	50	trace	-	-	-	-	-
15	Al^iBu_3	100	trace	-	-	-	-	-
16	$Ph_3C^+[B(C_6F_5)_4]^-$/ TIBA	50[d]	71.9	2.9	91.2	5.9	10.5	2.7
17	$AlEt_2Cl$	50	97.2	1.5	96.9	1.6	14.1	2.2
18	$AlEt_2Cl$	100	97.4	1.6	97.0	1.4	15.9	2.2
19	$Al_2Et_3Cl_3$	50	95.3	0.9	98.1	1.0	10.2	2.8
20	$Al_2Et_3Cl_3$	100	97.5	1.2	97.2	1.6	9.5	2.4

Polymerization conditions: toluene, 20 mL; butadiene, 0.1 mmol; precursor, 0.05 mmol; reaction temperature, room temperature, [a] at 0°C, [b] at 38°C and [c] at 55°C, [d] $Ph_3C^+[B(C_6F_5)_4]^-$/Co =1.0, TIBA/Co = 50, polymerization time, 4h.

Table 4 The phosphine effect on the catalytic performance of the cobalt catalyst

Run	Phosphine (P)	[P]/ [Co]	Yield (%)	Microstructure (%)			M_n (10^4)	PDI
				Trans-1,4	*Cis*-1,4	1,2		
21	PPh_3	0.1	85.5	7.8	63.2	29.0	9.0	2.6
22	PPh_3	0.3	59.2	9.4	50.1	40.5	9.9	2.5
23	PPh_3	0.6	78.8	7.6	30.1	62.3	9.7	2.5
24	PPh_3	1.0	88.3	3.1	13.3	83.6	9.2	2.1
25	PPh_3	1.2	90.0	3.7	13.9	82.4	11.0	2.3
26	PPh_3	1.5	90.5	3.8	13.2	83.0	11.1	2.5
27	PEt_3	1.0	56.5	3.5	79.4	17.1	7.4	2.7
28	PCy_3	1.0	73.2	10.9	60.4	28.7	8.7	2.9

Polymerization conditions: toluene, 20 mL; butadiene, 0.1 mol; **Co(II)Cl_2L**, 0.05 mmol; reaction temperature, room temperature, [a] at 0°C, [b] at 50°C, polymerization time, 4h.

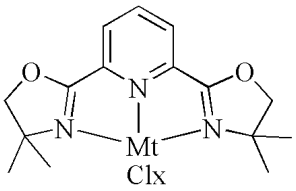

MtClx = $CrCl_3$ (**C1**), $FeCl_3$(**C2**), $FeCl_2$(**C3**), $CoCl_2$(**C4**).

Fig. 1 2,6-Bis(dimethyl-2-oxazolin-2-yl)pyridine supported **Cr(III)Cl_3L**, **Fe(III)Cl_3L**, **Fe(II)Cl_2L** and **Co(II)Cl_2L** complexes

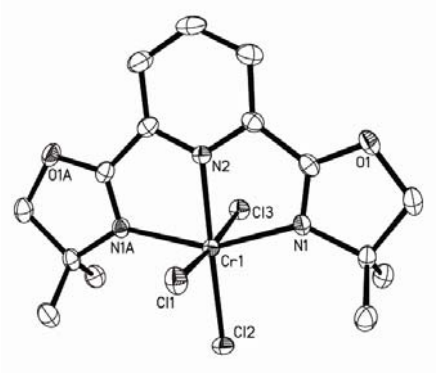

Fig. 2 ORTEP drawing of complex **Cr(III)Cl_3L** with thermal ellipsoids at 30% probability level. Hydrogen atoms have been omitted for clarity.

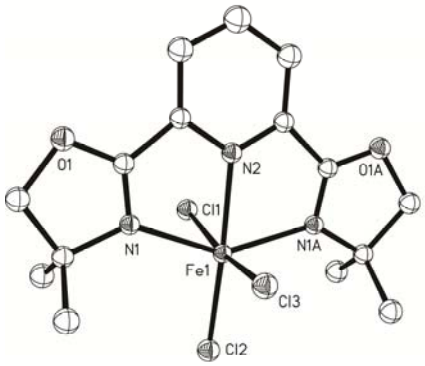

Fig. 3 ORTEP drawing of complex **Fe(III)Cl_3L** with thermal ellipsoids at 30% probability level. Hydrogen atoms have been omitted for clarity.

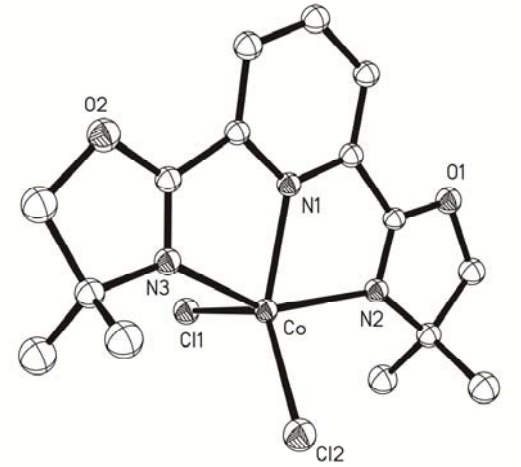

Fig. 4 ORTEP drawing of complex **Co(II)Cl_2L** with thermal ellipsoids at 30% probability level. Hydrogen atoms have been omitted for clarity.